Hypoglycaemia combined with mild hypokalaemia reduces the heart rate and causes abnormal pacemaker activity in a computational model of a human sinoatrial cell

Alan Bernjak[a,b], Ahmed Iqbal[a,c], Simon R Heller[a,c], Richard H Clayton[d,b]

[a]Department of Oncology & Metabolism, University of Sheffield, Sheffield, United Kingdom, [b]INSIGNEO Institute for *in silico* Medicine, University of Sheffield, Sheffield, United Kingdom, [c]Sheffield Teaching Hospitals NHS Foundation Trust, Sheffield, United Kingdom, [d]Department of Computer Science, University of Sheffield, Sheffield, United Kingdom

Corresponding author:

Alan Bernjak, Research Associate

Department of Oncology & Metabolism, University of Sheffield, Medical School, Beech Hill

Road, Sheffield, S10 2RX, United Kingdom, e-mail: a.bernjak@sheffield.ac.uk, ORCID iD:

0000-0001-5954-8079

No. of Figures: 10 (+ 3 Supplementary Figures)

No. of Tables: 2

Abstract

Low blood glucose, hypoglycaemia, has been implicated as a possible contributing factor to sudden cardiac death (SCD) in people with diabetes but it is challenging to investigate in clinical studies. We hypothesised the effects of hypoglycaemia on the sinoatrial (SA) node in the heart to be a candidate mechanism and adapted a computational model of the human SA node action potential developed by Fabbri et al, to investigate the effects of hypoglycaemia on the pacemaker rate. Using Latin hypercube sampling, we combined the effects of low glucose on the hERG channel with reduced blood potassium, hypokalaemia and added sympathetic and parasympathetic stimulus. We showed that hypoglycaemia on its own causes a small decrease in heart rate but there was also a marked decrease in heart rate when combined with hypokalaemia. The effect of the sympathetic stimulus was diminished, causing smaller increase in heart rate, with low glucose and hypokalaemia compared to normoglycaemia. In contrast, the effect of the parasympathetic stimulus was enhanced, causing greater decrease in heart rate. We therefore demonstrate a potential mechanistic explanation for hypoglycaemia-induced bradycardia and show that sinus arrest is a plausible mechanism for SCD in people with diabetes.

Abbreviations:

AP - action potential

APA – action potential amplitude

APD_{90} – action potential duration at 90% repolarisation

bpm – beats per minute

CL – pacemaker cycle length

DDR - diastolic depolarisation rate

DDR_{100} – early (first 100ms) diastolic depolarisation rate

g_{Kr} – normalised conductance of the delayed rectifier potassium current (I_{Kr})

Glu_o – extracellular glucose concentration

IVshift – shift in the current-voltage relationship of I_{Kr}

hERG channel – human ether-a-go-go-related gene (HERG) potassium channel

K_o - extracellular potassium concentration

MDP - maximum diastolic potential

PP - peak action potential

SAN – sinoatrial node

SCD – sudden cardiac death

NG – normoglycaemia

LG – low glucose

Introduction

Blood glucose levels are elevated in both type 1 and type 2 diabetes. Insulin is used to therapeutically lower high glucose in individuals with type 1 and long-standing type 2 diabetes, however, this commonly results in iatrogenic hypoglycaemia; one major barrier in achieving and maintaining normal glucose control in diabetes (1). Insulin causes glucose to fall, but in individuals with diabetes, insulin levels are reduced both due to auto-immune damage to the pancreatic β cells (type 1 diabetes) or a combination of impaired insulin secretion and action (type 2 diabetes). In both types of diabetes, exogenous insulin is used to lower glucose therapeutically but due to the limitations of current insulin delivery, insulin replacement is unphysiological. It is challenging to achieve stable basal concentrations and those with insulin treated diabetes are subject to both hyper-and hypoglycaemia. Attempts to mimic normal glucose levels through intensive insulin therapy increase the risk of severe hypoglycaemic episodes. The effects of hypoglycaemia on the cardiovascular system have only recently emerged and severe hypoglycaemia has been associated with increased mortality in randomised trials (2,3). In one of the trials, intensive glucose therapy resulted in a six-fold increase in severe hypoglycaemia (2). Over one third of deaths were attributed to sudden cardiac death (SCD), raising the possible link between hypoglycaemia and cardiac arrhythmias.

Indeed, there is growing evidence in recent clinical and animal studies that hypoglycaemia might contribute to malignant cardiac arrhythmias leading to SCD. Severe hypoglycaemia in response to glucose therapy was associated with increased risk of arrhythmic death in individuals with type 2 diabetes (3). Spontaneous nocturnal hypoglycaemia was also implicated in the deaths of young people with type 1 diabetes. The term 'dead in bed syndrome' was introduced to describe these unexpected deaths (4), which were attributed to SCD. Subsequent studies reported a relatively large proportion of unexplained deaths in this population (5,6). Although rare in absolute numbers, SCD is 10-fold higher in young people with type 1 diabetes compared to those without diabetes (7). In observational studies, we and others reported increased risk of arrhythmias, including slow heart rate, bradycardia, during spontaneous hypoglycaemia versus normoglycaemia (8–11). These arrhythmias could be related to abnormal cardiac repolarisation observed in spontaneous (12) and experimental hypoglycaemia studies, where hypoglycaemia was induced by infusion of insulin (13–15). Experimental hypoglycaemia in rats can cause lethal cardiac arrhythmias, although at glucose levels significantly lower compared to those in human studies (16).

Possible hypoglycaemia-induced proarrhythmic mechanisms include the direct effect of low extracellular glucose on the myocardial cell, which can block potassium channels that carry an outward current during repolarisation (17). This causes a prolongation in the cardiac action potential as well as lengthening of the QT interval duration in the ECG through a mechanism identical to that in proarrhythmic medications (18). In addition, the counterregulatory sympathoadrenal activation in response to hypoglycaemia causes a release of adrenaline (19), which in turn lowers serum potassium concentration (20) and increases intracellular calcium concentration (21). Combined, these can cause further QT interval prolongation and calcium

overload and lead to proarrhythmogenic electrical instability (21). Abnormal autonomic responses which are common in diabetes could cause further risk in these individuals.

The autonomic response to falling glucose levels includes sympathetic and parasympathetic activation, with the latter limiting the increase in heart rate during hypoglycaemia. However, bradycardia was also observed during spontaneous (22) and experimental hypoglycaemia (23). In our observational studies, we detected increased rates of bradycardia during hypoglycaemia compared to normoglycaemia in some individuals with diabetes (8,10,11). Bradycardia was also common during experimental hypoglycaemia in rats (16). These observations suggest that bradycardia might be an additional risk factor during hypoglycaemia, possibly by development of early afterdepolarisations leading to ventricular tachycardia, particularly in the presence of hypokalaemia (24). Our focus in this study was therefore on the effect of hypoglycaemia on the sinoatrial node (SAN), the heart's natural pacemaker.

Hypoglycaemia studies present challenges to investigators. While hypoglycaemia and cardiac arrhythmias are relatively common, SCD is rare, suggesting the involvement of additional factors, including variable and dysfunctional autonomic responses and impaired awareness of hypoglycaemia. Observational clinical hypoglycaemia studies are limited by an inability to measure electrolytes and catecholamines during spontaneous episodes of hypoglycaemia. Experimental studies on the other hand while more controlled, require supra-physiological concentrations of insulin to induce hypoglycaemia, rarely encountered in clinical practice. In addition, a greater fall in potassium in these studies is not representative of what happens in people with diabetes in the 'free living' condition. Animal models offer an alternative approach but species differences in the hormonal responses to hypoglycaemia and ensuing cardiac electrophysiological responses mean there are limitations in drawing conclusions from these data.

In this study we have therefore used a computational model to overcome some of these limitations. There are currently no computational models that describe the electrophysiological responses to hypoglycaemia and in this study, we adapted a biophysically detailed computational model of a human SAN cell electrophysiology to examine the effect of hypoglycaemia on pacemaker rate.

Methodology

Model of the human sinoatrial node AP

We used a computational model of the human SAN action potential (AP), developed by Fabbri et al (25). This model was in turn adapted from a computational rabbit SAN model, developed by Severi et al (26) by incorporating experimental data from human SAN cells. These included updated cell capacitance and dimension data, new formulation of the I_f current, new steady-state activation and updated conductances of delayed rectifier K$^+$ currents (I_{Kr} and I_{Ks}) and added I_{Kur} current formulation. Parameters, for which human experimental data were not available, were fitted using automatic parameter optimisation. The modulation of the pacemaker rate in response to autonomic stimulation was similarly adapted from the rabbit model, where acetylcholine

(ACh)- and isoprenaline (Iso)-induced variations were introduced to mimic the activation of the sympathetic (increased rate) and parasympathetic (decreased rate) nervous system, respectively. Further details about the model are provided in Supplementary Material.

We ran simulations in MATLAB (The MathWorks, Inc., Natick, MA, USA) vR2017a, using automatically generated code for the Fabbri model obtained from the CellML platform (www.cellml.org). For solving numerical differentiation, we used the 'ode15s' function with relative error tolerance 10^{-7}, absolute error tolerance 10^{-6} and a maximum step size of 10^{-3}s. We ran the simulations for 60s and used the last beat to calculate the features of AP waveforms and for figures. We confirmed the stability of the main features of the AP waveform (Supplementary Figure 1).

Features of sinoatrial AP waveform

We characterised the sinoatrial AP waveform using a set of parameters presented by Fabbri et al and we calculated them based on the guidelines for standardisation of AP parameters (27). The following parameters were calculated: CL – cycle length of the pacemaker activity, defined as the duration between the peaks of two consecutive APs; PP – peak (maximum value) of the AP; APA – AP amplitude, defined as the difference between the maximum and minimum AP potentials; MDP – maximum diastolic potential preceding the PP, defined as the most negative repolarisation potential, DDR – diastolic depolarisation rate, DDR_{100} – diastolic depolarisation rate over the first 100ms of diastolic depolarisation, APD_{90} – AP duration at 90% repolarisation (Figure 1).
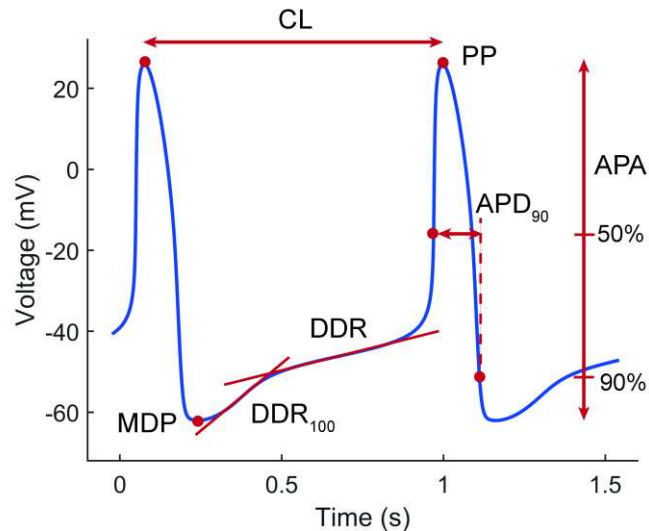

Figure 1: Features of the sinoatrial AP waveform. CL – cycle length; PP – peak potential; APA – AP amplitude; MDP – maximum diastolic potential; DDR – diastolic depolarisation rate; DDR_{100} – early diastolic depolarisation rate; APD_{90} – AP duration at 90% repolarisation.

The main parameter of our interest was CL. We explored the changes induced by hypoglycaemia and the main features of AP responsible for these changes.

Effect of low extracellular glucose – experimental data

In an experimental study, Zhang et al demonstrated a direct effect of low extracellular glucose concentration (Gluo) on the rapid delayed rectifier potassium current (I_{Kr}) (17). Using a whole-cell patch clamp they showed an impairment in the function of the corresponding hERG channel, proportional to the reduction in Gluo. Zhang et al used human embryonic kidney cells (HEK293 cells) and in this study we assume that electrophysiological properties and responses of the hERG channels are similar in the heart, where hERG is highly expressed.

Zhang et al demonstrated two separate mechanisms by which reduced Gluo alters the function of the hERG channel: a reduction in I_{Kr} current density and a shift in its current-voltage relationship. We digitised their graphs to numerically quantify the extent of changes. We further describe the effect size for both mechanisms and how we incorporated them in our model.

Reduced I_{Kr} current density

Zhang et al presented experimental data for I_{Kr} voltage-current relationships at various extracellular glucose concentrations: Gluo=5 (normoglycaemia), 2.5, 1, and 0mmol/L. They demonstrated a 10-20% reduction in current density at Gluo=2.5mmol/L compared to 5mmol/L, a 20-30% reduction at 1mmol/L and a 50% reduction at 0mmol/L. The current density decreased proportionally with decreased Gluo, but the reduction was not constant across the voltage range. In our model, we incorporated the drop in current density by decreasing the conductance (g_{Kr}) of I_{Kr}. For easier interpretation, g_{Kr} in our model represents normalised conductance, a multiplier of maximum conductance (4.2nS in the Fabbri model). We decreased g_{Kr} from 1 (maximum conductance, no effect of glucose) to 0 to investigate the overall response of the model. We then varied g_{Kr} within the [1, 0.7] range (100% to 70% of maximum conductance) to consider only physiologically relevant glucose concentrations, based on the above data.

Shift in the I_{Kr} current-voltage relationship (IVshift)

Zhang et al demonstrated that the I_{Kr} current-voltage (I-V) relationship shifted towards more negative potentials with reduced Gluo. Specifically, they reported a -10mV shift at Gluo = 0 vs 5mmol/L. There was a similar -10mV shift in normalised conductance. I-V relationships were not shown for other Gluo, but they performed additional experiments under conditions with corrected osmolarity at Gluo=1mmol/L. In these experiments they measured a -3mV shift in normalised conductance at Gluo = 1 vs 5 mmol/L and for the purpose of our study we assumed that the shift in I-V curves is similar. This is since the shifts in the I-V relationship and conductance were similar in the experiment without correction for osmolarity. To model physiologically relevant effects of hypoglycaemia we varied IVshift within [-3, 0]mV range but we explored shifts below -3mV to test the overall response of the model.

We extracted all relevant data by digitising the graphs and we measured the shifts at 50% I-V curve or conductance amplitude. In the Fabbri model, I_{Kr} is formulated as a function of membrane potential by combining the activation and inactivation kinetics. To model the shift in the I-V curve we incorporated IVshift into the membrane potential variables of all equations describing the activation and inactivation relationships and their corresponding time constants.

Latin hypercube sampling

We used Latin hypercube sampling for simulations where two or more input parameters were randomly selected from a predefined range. The sampling was performed by using the 'lhsdesign' algorithm in MATLAB. The variable input parameters included g_{Kr}, IVshift and extracellular potassium concentration (Ko).

Outline of the study

We investigated the individual effect of each parameter g_{Kr}, IVshift and Ko on CL and features of the AP waveform. For each parameter, the modelling was performed for physiologically relevant values as well as outside this range to test the behaviour of the model and to identify input values that produce meaningful APs. We also looked at the combined effects of these parameters when their values were within physiologically relevant ranges. Using Latin hypercube sampling we varied g_{Kr} (g_{Kr} is a multiplier of maximum conductance) between 0.7 and 1, IVshift between -3 and 0mV and Ko between 3.0 and 4.0mmol/L. Ko at 4.0mmol/L represents normal extracellular potassium concentration while Ko=3.0mmol/L indicates moderate hypokalaemia. Finally, we checked the combined effect of these parameters with additional activation of either the sympathetic or parasympathetic autonomic system. The current model allows only one of them to be activated at any time.

Results

Baseline sinoatrial AP waveform

Fabbri et al fitted and optimised their model at Ko=5.4mmol/L, resulting in CL=0.81s (rate=74bpm). For the purpose of our study we changed the baseline Ko to 4.0mmol/L, closer to normal plasma potassium range in humans which is between 3.5 and 5mmol/L (28). This resulted in prolonged CL=0.92s (13.5% increase, 65 vs 74bpm), which was mostly caused by decreased DDR_{100} (40.1 vs 56.0, -28%) and lower MDP (-62.0 vs -58.9mV, -5%). The AP waveform at normoglycaemia (NG) and Ko=4.0mmol/L is presented in Figure 1 and its features at Ko=5.4 and Ko=4.0mmol/L are given in Table 1. Throughout the results section, percentage changes in parameters are given compared to baseline levels at Ko = 4.0mmol/L.

	NG			LG			LG + low Ko		
g_{Kr}	1	1	1	0.7	1	0.7	0.7	1	0.7
IVshift (mV)	0	0	0	0	-3	-3	0	-3	-3
Ko (mmol/L)	5.4	4.0	3.0	4.0	4.0	4.0	3.0	3.0	3.0
CL (s)	0.81	0.92	0.94	0.75	1.20	0.93	0.85	1.33	1.04
PP (mV)	26.4	25.9	25.5	27.3	25.7	27.5	27.1	24.8	27.1
APA (mV)	85.3	87.9	91.3	84.2	92.5	87.8	86.4	96.1	90.4
MDP (mV)	-58.9	-62.0	-65.8	-56.9	-66.8	-60.3	-59.3	-71.3	-63.3
APD$_{90}$ (s)	0.15	0.14	0.14	0.17	0.15	0.18	0.17	0.15	0.17
DDR	21.6	19.0	20.6	25.1	10.9	18.3	21.9	8.4	16.2
DDR$_{100}$	56.0	40.1	35.4	51.0	34.1	52.2	44.9	35.3	33.7

Table 1: Features of the AP waveform (rows 5 and onwards) calculated using a combination of input parameters (rows 2 to 4) representing normoglycaemia (NG), low glucose (LG) and a combination of LG and low potassium. Baseline values of input parameters (bold highlight), their extreme values and their combinations are considered. We changed the baseline Ko=5.4mmol/L in the Fabbri model to Ko=4.0mmol/L.

Effect of low glucose

Reduced conductance of the hERG channel

We reduced g_{Kr} (g_{Kr} is a multiplier of maximum conductance) from 1 (maximum conductance) to 0 in steps of 0.05. The model failed to generate spontaneous AP activity at g_{Kr}<0.11. The relationship between g_{Kr} and CL is presented in Figure 2a. CL shortens with decreased g_{Kr} and the relationship is approximately linear down to g_{Kr}=0.4, followed by a plateau. The minimum CL at g_{Kr}=0.11 is 0.47s (-49%). The vertical blue lines indicate the [0.7, 1] range, which represents our estimated reduction in g_{Kr} at clinically relevant reduced glucose concentrations. CL at g_{Kr}=0.7 is 0.75s (-18%), APD is prolonged (+21%), the MDP potential is elevated (+8%) and the diastolic depolarisation rates DDR and DDR$_{100}$ are increased (+32% and +27%) (Table 1). Examples of the corresponding AP waveforms are presented in Figure 2b.
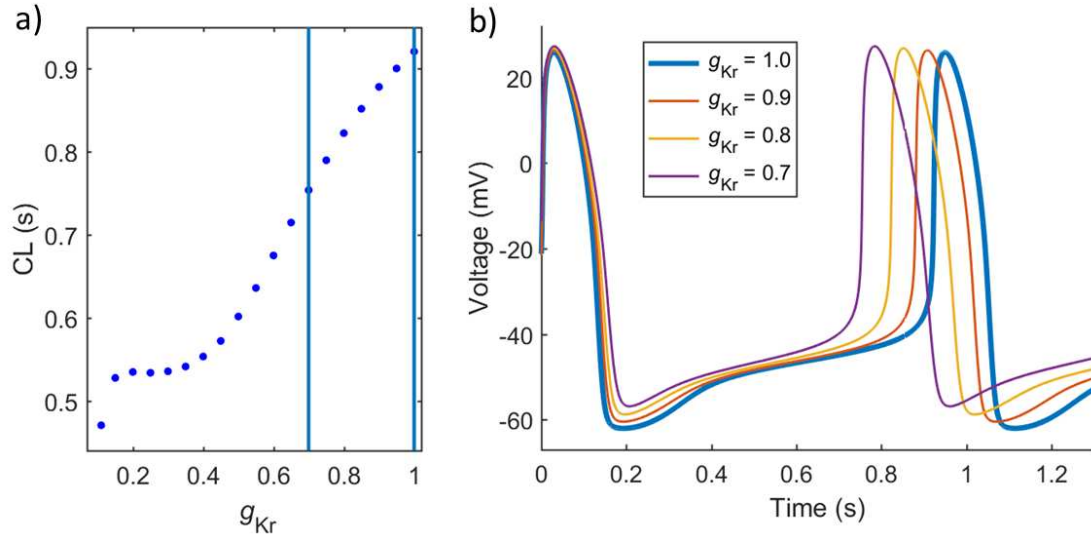
Figure 2: Effect of reduced g_{Kr} on the AP waveform. a) Relationship between g_{Kr} and CL. Vertical lines indicate the g_{Kr} range at clinically relevant glucose concentrations. b) AP waveforms demonstrating shortened CL (increased rate), prolonged APD, elevated MDP and increased DDR with a decrease in g_{Kr}.

Negative shift in I_{Kr} current-voltage relationship

We introduced a negative shift (towards more negative potentials) in the I-V relationship (IVshift), starting from 0mV in steps of -0.1mV. CL exponentially increases with negative IVshift (Figure 3a) and the longest valid CL is obtained at -5.4mV (CL=5.94s). The blue vertical lines indicate the [-3, 0]mV range which represents our estimated shift at clinically relevant glucose concentrations. CL at IVshift=-3mV equals 1.2s (+30%) and the prolongation is mostly caused by decreased MDP (-8%) and depolarisation rates DDR (-43%) and DDR_{100} (-15%) (Table 1). The corresponding AP waveforms are presented in Figure 3b.
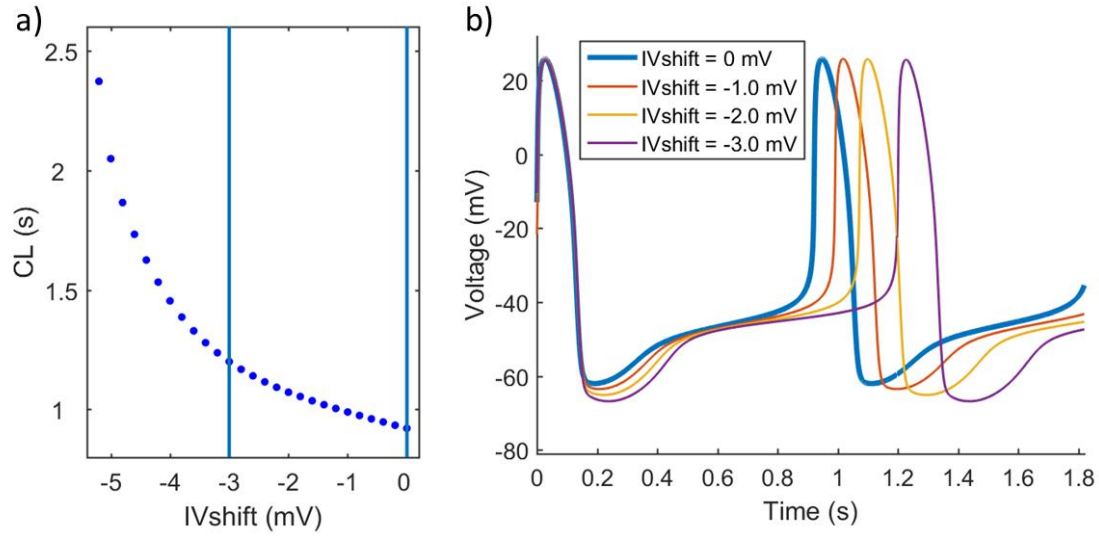
Figure 3: Effect of negative IVshift on the AP waveforms. a) Relationship between CL and IVshift. The blue vertical lines indicate our estimated range of IVshift at clinically relevant glucose concentrations. b) AP waveforms showing gradual CL prolongation with IVshift, mostly caused by decreased MDP and DDR/DDR$_{100}$.

Combined effects of reduced g_{Kr} and negative IVshift

We combined the effects of reduced g_{Kr} and negative IVshift by simultaneously sampling g_{Kr} from [0.7, 1] and IVshift from [-3, 0]mV ranges. We used Latin hypercube sampling to generate 300 pairs of random and independent input variables for 300 evaluations of the model. The resulting CLs are presented in Figure 4. Red data indicate CL prolongation and blue data CL shortening versus baseline (CL=0.92s) (Figure 4a). CLs are longest at baseline g_{Kr} (g_{Kr}=1) combined with maximum IVshift (IVshift=-3mV) and are shortest at g_{Kr}=0.7 combined with baseline IVshift (0mV). The grey dashed line indicates simultaneous linear change in both parameters. CLs along this line are approximately constant and are slightly longer than baseline CL (~0.93s. +1%). In Figure 4b a projection of CL values to the g_{Kr} axis shows a gradual shortening of CL with decreased g_{Kr}, and for each g_{Kr}, CL is prolonged with the negative IVshift. The maximum and minimum CLs obtained with these parameters are 1.2s (+30%) and 0.75s (-18%), respectively (Table 1).
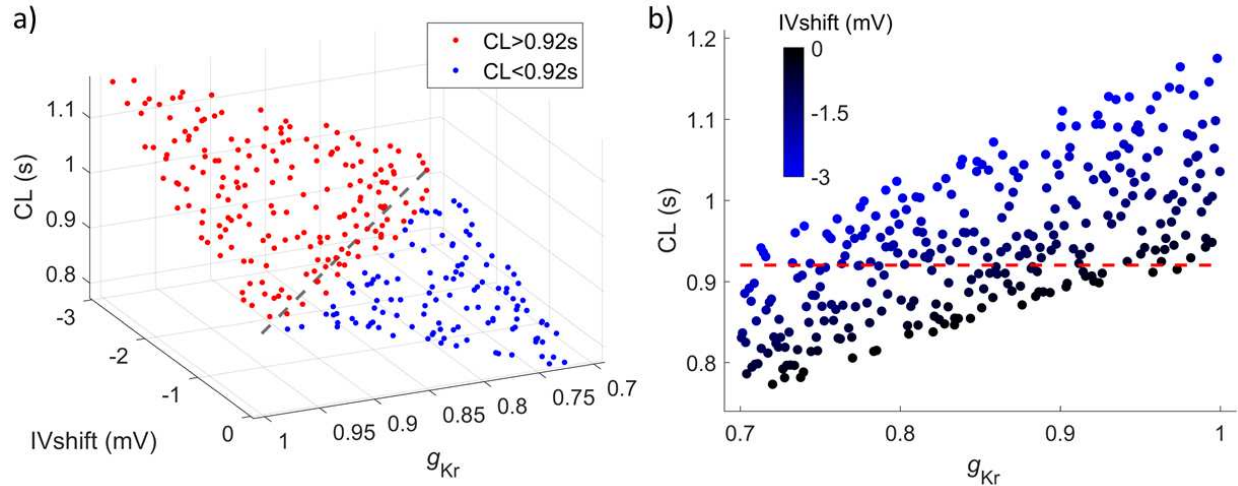
Figure 4: Combined effects of reduced g_{Kr} ([0.7, 1]) and negative IVshift ([-3, 0]mV) on CL, using Latin hypercube sampling (n=300). a) CL as a function of g_{Kr} and IVshift. Red data indicate CL prolongation and blue data CL shortening vs baseline (CL=0.92s). The grey dashed line indicates a linear change in both parameters. b) A projection to the g_{Kr} axis reveals gradual shortening of CL with reduced g_{Kr}. At each g_{Kr}, CL is prolonged with negative IVshift. The red dashed line shows baseline CL.

1. Features of the AP waveform

The individual effects of reduced g_{Kr} and negative IVshift produce CL changes in opposite directions (Figure 2) and their combined effects cancel each other out to some degree, producing a slight CL prolongation. A similar opposite effect is obtained with other AP features, including APA, MDP and DDR. For example, baseline MDP equals -62.0mV (Table 1) and the combined effects of g_{Kr}=0.7 and IVshift=-3mV slightly raise MDP to -60.3mV (+3%). Individual changes in g_{Kr} and IVshift however produce a bigger difference compared to baseline with minimum/maximum MDP values -66.8mV (-8%) and -56.9mV (+8%), respectively. On the other hand, PP, APD$_{90}$ and DDR$_{100}$ are predominantly affected by one of the input parameters but not by the other. For these AP features, the combined changes in g_{Kr} and IVshift produce values outside the range of their individual effects. For example, APD$_{90}$ is prolonged at g_{Kr}=0.7 (APD$_{90}$=0.17s, +21%) but with added IVshift=-3mV there is a further prolongation (APD$_{90}$=0.18s, +29%). Maximum values of PP, ADP$_{90}$ and DDR$_{100}$ are achieved when both g_{Kr} and IVshift are at the maximum of their ranges.

Effect of low extracellular potassium

With the other input parameters at baseline (normoglycaemia), we lowered Ko from 5mmol/L in steps of -0.1mmol/L. The relationship between Ko and CL is presented in Figure 5a in blue color. The lowest Ko that produces periodic pacemaker activity is 0.6mmol/L (CL=1.54s, +67%). CL is slightly prolonged with the decrease in Ko from 4mmol/L to 3mmol/L (blue vertical lines) and reaches a local maximum of 0.94s (+2%) at 3.3mmol/L. The prolongation is

mainly caused by more negative MDP (-6%) and decreased DDR_{100} (-12%) (Figure 5c and Table 1).
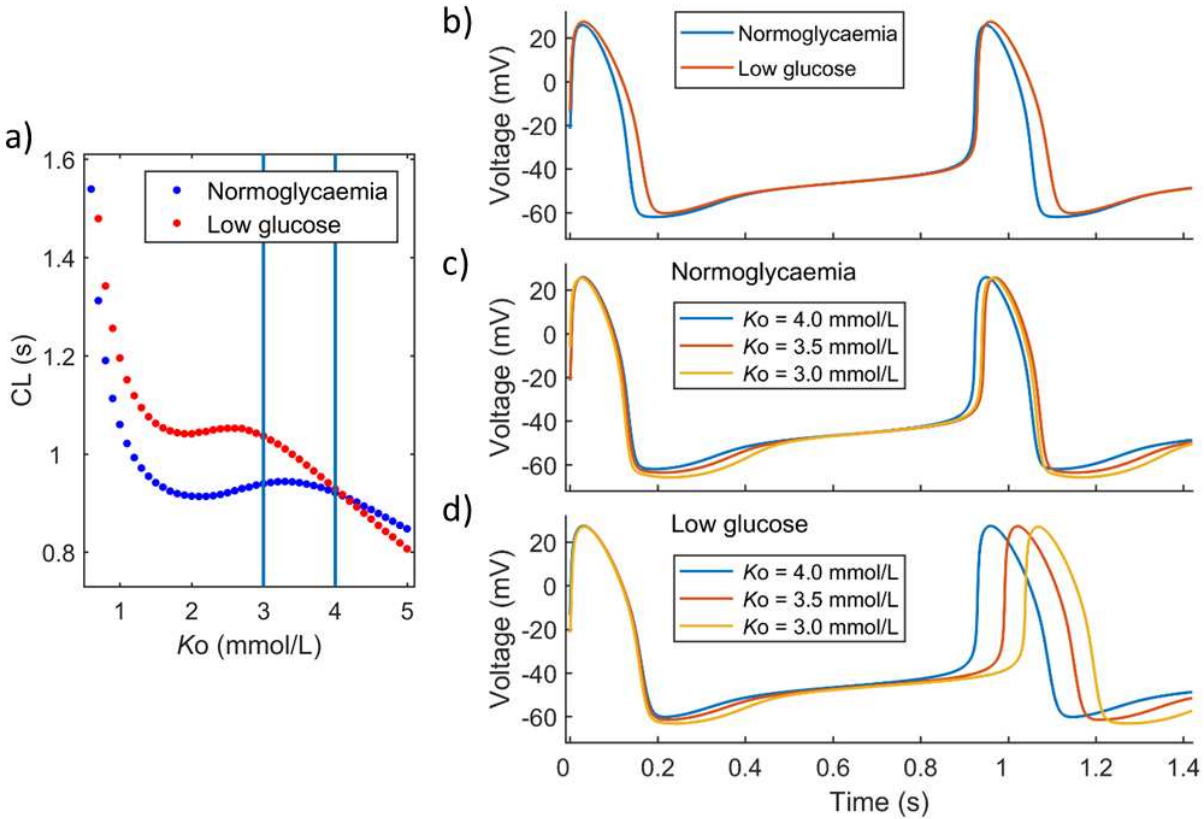

Figure 5: Effect of reduced Ko on CL. a) Relationship between Ko and CL at normoglycaemia (g_{Kr}=1, IVshift=0mV, blue) and at low glucose (g_{Kr}=0.7, IVshift=-3mV, red). b) AP waveforms at normoglycaemia and low glucose (both at Ko=4mmol/L). c) Effect of reduced Ko on AP waveforms is small during normoglycaemia. d) Reduced Ko combined with low glucose produces a relatively big prolongation in CL.

Combined effects of low Gluo and Ko

We first combined the effects of low Gluo and Ko by fixing g_{Kr} and IVshift at the maximum of their ranges: g_{Kr}=0.7, IVshift=-3mV and by reducing Ko in a stepwise manner. Second, we randomly sampled all three parameters (g_{Kr}, IVshift and Ko) from their predefined ranges.

Fixed g_{Kr} and IVshift, combined with stepwise reduced Ko

With g_{Kr} and IVshift fixed at 0.7 and -3mV respectively, we decreased Ko from 5mmol/L in steps of -0.1mmol/L. The relationship between CL and Ko is presented in Figure 5a (red). In contrast to normoglycaemia (blue), the relationship is steeper for Ko between 3 and 5mmol/L

and there is a local maximum at K_o=2.6mmol/L (CL=1.05s, +14%). At K_o =4mmol/L, CL is similar at normoglycaemia and low glucose (0.92s vs 0.93s, +1%) but with reduced K_o=3mmol/L there is a notable prolongation in CL at low glucose (CL=1.04s, +13%) vs normoglycaemia (CL=0.94s, +2%). The corresponding AP waveforms are presented in Figure 5b-d. Low glucose causes APD prolongation (0.18s, +29%) with a minor effect on CL (0.93s, +1%) (b). Reduced potassium at normoglycaemia produces a slight prolongation in CL (c) but the prolongation is substantially greater when combined with low glucose (d) (CL data are given above).

Randomly sampled g_{Kr}, IVshift and Ko

We randomly varied g_{Kr}=[0.7, 1], IVshift=[-3, 0]mV and K_o=[3, 4]mmol/L using Latin hypercube sampling by generating 2000 independent evaluations of the model. The resulting CLs are presented in Figure 6. In panel a, red data designate the area of input parameters which cause CL prolongation and blue data the area resulting in CL shortening versus baseline. The grey panel indicates a linear change in g_{Kr} and IVshift. At K_o=4mmol/L, the model generates both prolongation and shortening of CL. With reduced K_o, the number of cases resulting in CL shortening is decreasing proportionally and at K_o=3mmol/L these are confined to the subspace g_{Kr}<0.8 and IVshift>-1mV. In panel b, absolute values of CL are presented (grey) as a function of K_o. There is a relatively broad spread of CL but also a systematic CL prolongation with reduced K_o. At K_o=3mmol/L most of the evaluations of the model result in CL prolongation vs baseline (red dashed line). For reference, data at normoglycaemia are shown (blue), as well as at low glucose with g_{Kr} and IVshift fixed at 0.7 and -3mV, respectively (red). The shortest CL is 0.76s (-17%) at g_{Kr}=0.7, IVshift=0mV and K_o = 3.92mmol/L and the longest CL is 1.28s (+39%) at 1, -3mV and 3.1mmol/L, respectively. By combining the effects of randomly sampled input parameters, CL stays within the range obtained from parameters at the extreme ends of their predefined ranges (Table 1).
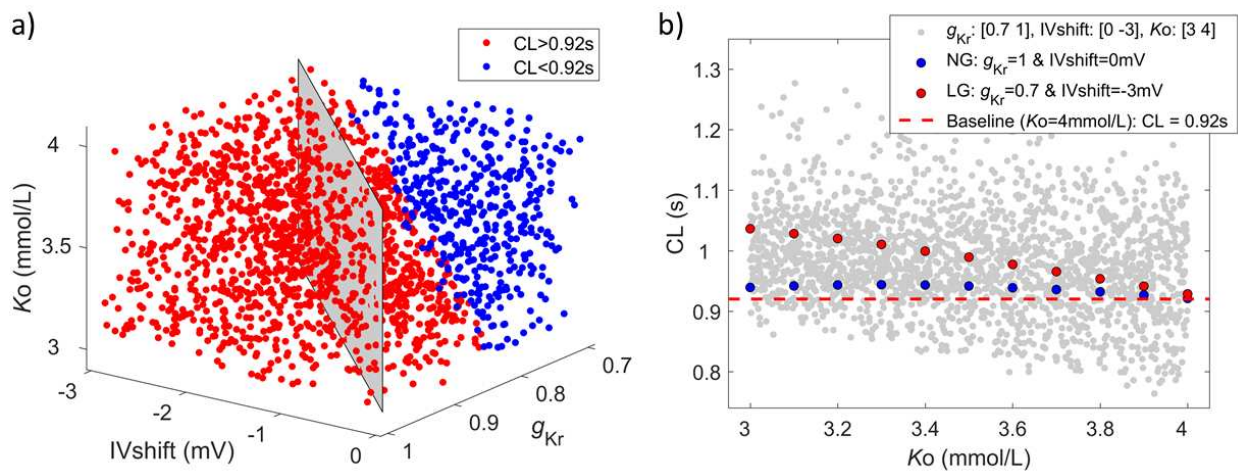

Figure 6: Combined effects of low glucose and low potassium on CL using randomly sampled g_{Kr} ([0.7, 1]), IVshift ([-3, 0]mV) and K_o ([3, 4]mmol/L). a) Red data indicate CL prolongation

and blue data CL shortening vs baseline (CL=0.92s). A linear change in g_{Kr} and IVshift (grey panel) causes CL prolongation which increases with decreased Ko. b) Range of CL values for random input parameters (grey). Blue data show the relationship with Ko at normoglycaemia and red data at low glucose (LG) when g_{Kr} and IVshift are fixed at their extremes (g_{Kr}=0.7, IVshift=-3mV). Latin hypercube sampling, n=2000.

Autonomic modulation

We investigated the effect of autonomic modulation by separately including in the model either sympathetic or parasympathetic activity. In both scenarios we looked at the combined responses of autonomic activity, low glucose, and low potassium. To model low glucose, we first fixed g_{Kr} and IVshift at the extreme ends of their ranges. Second, we explored all possible outcomes by randomly sampling all input parameters (g_{Kr}, IVshift and Ko).

Fixed g_{Kr} and IVshift

At NG and Ko=4mmol/L, an addition of sympathetic activity shortens the CL from 0.92s to 0.69s (-25%). In Figure 7a, the grey dashed line shows the AP at NG without and the blue line with added sympathetic activity. Low glucose (g_{Kr}=0.7 and IVshift=-3mV) combined with sympathetic activity further shortens the CL (0.64s, -30%, red line). An additional reduction in Ko causes CL prolongation, reaching 0.70s (-24%) at Ko=3.5mmol/L (yellow) and 0.78s (-15%) at Ko=3mmol/L (purple).

An addition of parasympathetic activity at NG causes CL prolongation from 0.92s (Figure 7b, grey dashed line) to 1.27s (+38%) (blue). Low glucose combined with parasympathetic activity further prolongs the CL (1.36s, +48%, red). An additional reduction in Ko causes a further relatively big prolongation: CL=1.52s (+65%) at Ko=3.5mmol/L (yellow) and CL=1.73s (+88%) at Ko=3mmol/L (purple). The features of the AP waveforms are given in Table 2 and the relationship between CL and Ko at NG and LG is presented in Figure 8 using blue and red colors, respectively.

In the simulations including sympathetic and parasympathetic activity, a reduction in Ko combined with LG causes CL prolongation, predominantly caused by decreased rates of diastolic depolarisation (DDR and DDR_{100}) (Table 2). When combined with sympathetic activity, DDR and DDR_{100} are decreased by -23% (18.5 vs 23.9) and -22% (59 vs 67) at LG and Ko=3mmol/L vs LG and Ko=4mmol/L. The reductions are greater, -33%, (6.2 vs 9.3) and -38%, (25.1 vs 40.5) when combined with parasympathetic activity.
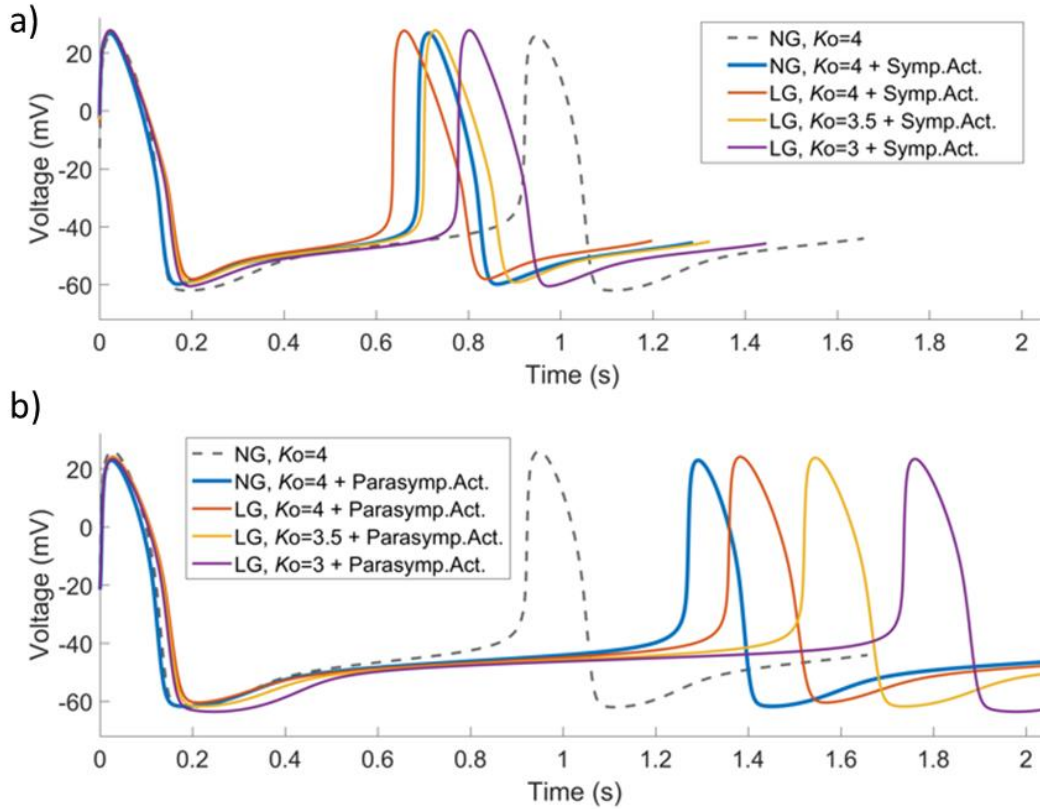
Figure 7: AP waveforms at NG and low glucose (LG: g_{Kr}=0.7 and IVshift=-3mV) in combination with reduced Ko and activation of either a) sympathetic activity (Symp.Act) or b) parasympathetic activity (Parasymp.Act.). In both cases, reduced Ko at LG causes gradual CL prolongation.

	NG	**+Sympathetic Act.**			**+Parasympathetic Act.**		
		NG	LG	LG+ Low Ko	NG	LG	LG+ Low Ko
g_{Kr}	**1**	**1**	0.7	0.7	**1**	0.7	0.7
IVshift (mV)	**0**	**0**	-3	-3	**0**	-3	-3
Ko **(mmol/L)**	**4.0**	**4.0**	**4.0**	3.0	**4.0**	**4.0**	3.0
CL (s)	**0.92**	0.69	0.64	0.78	1.27	1.36	1.73
PP (mV)	**25.9**	26.8	27.6	27.8	22.8	24.1	23.3
APA (mV)	**87.9**	*86.6*	85.7	*88.3*	84.6	84.5	86.9
MDP (mV)	**-62.0**	-59.8	-58.7	-60.5	-61.7	-60.4	-63.6
APD$_{90}$ (s)	**0.14**	0.14	0.17	0.17	0.14	0.17	0.16
DDR	**19.0**	21.9	23.9	18.5	10.4	9.26	6.22
DDR$_{100}$	**40.1**	58.3	67.0	59.0	34.0	40.5	25.1

Table 2: Features of AP waveforms at normoglycaemia (NG), low glucose (LG), and LG combined with low Ko (LG+Low Ko) with added either sympathetic or parasympathetic activity. Baseline values of input parameters (g_{Kr}, IVshift and Ko) and AP waveform features are highlighted in bold.

Randomly sampled g_{Kr}, IVshift and Ko

We used the existing 2000 random sets of input parameters g_{Kr}, IVshift and Ko, presented in Figure 6 and evaluated the model by adding either sympathetic or parasympathetic activity. The range of CL values, obtained after adding sympathetic activity is shown in Figure 8a (grey). For reference, the grey and red dashed lines indicate baseline CL at NG without (CL=0.92s) and with added sympathetic activity (CL=0.69s, -25%), respectively. The model produces valid periodic pacemaker activity with all sets of input parameters. The relationship between CL and Ko at normoglycaemia is further highlighted in blue and at low glucose (g_{Kr}=0.7, IVshift=-3mV) in red. The AP waveforms at Ko=3, 3.5 and 4mmol/L are presented in Figure 7a. There is a trend of CL prolongation with reduced Ko overall, as well as at NG and LG. For the whole range of Ko, CL is shorter at LG compared to NG (red data are below blue) and the difference is greatest at Ko=4mmol/L (CL=0.64s vs 0.69s, -7%).

The relationship between CL and Ko when combined with parasympathetic activity is shown in Figure 8b (grey). The grey and red dashed lines indicate baseline CL at NG without (CL=0.92s) and with added parasympathetic activity (CL=1.27s, +38%), respectively. There is a systematic CL prolongation with reduction in Ko. Some of the CLs are greater than 4s, especially at lower Ko, reaching CL~25s (data not shown). We show the distribution of the full extent of CL values on a logarithmic scale in Figure 8c. The relationship between CL and Ko at normoglycaemia is further highlighted in blue and at LG (g_{Kr}=0.7, IVshift=-3mV) in red. The AP waveforms at Ko=3, 3.5 and 4mmol/L are presented in Figure 7b. CL is prolonged with reduced Ko, but the prolongation is greater at LG vs NG (red data above blue), with the biggest difference at Ko=3mmol/L (CL=1.73s vs 1.50, +15%).

Some combinations of input parameters with added parasympathetic activity do not produce periodic pacemaker activity (data not presented, see below).
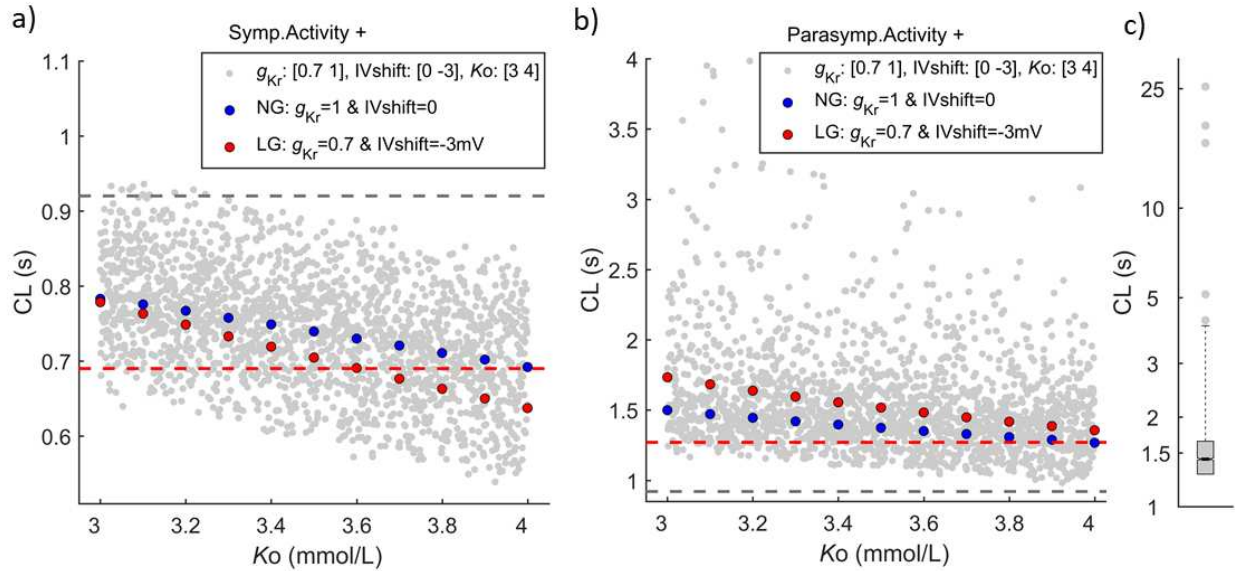
Figure 8: CL with randomly sampled g_{Kr} [0.7, 1], IVshift [-3, 0]mV and Ko [3, 4]mmol/L, using Latin hypercube sampling (N=2000) with the addition of either a) sympathetic activity or b,c) parasympathetic activity. Blue and red data present the relationship between CL and Ko at NG and at LG (g_{Kr}=0.7, IVshift=-3mV), respectively. Outlier CL values are not shown in panel b. The distribution of the full range is presented on logarithmic axis in panel c. Some combinations of input parameters combined with parasympathetic activity did not produce valid pacemaker activity (data not shown). The grey dashed lines show baseline CL at NG (CL=0.92s). The red dashed lines show CL at NG combined with (a) sympathetic activity (CL=0.69s) and (b) parasympathetic activity (CL=1.27s).

To identify input parameters which in combination with parasympathetic activity produce long CL or no pacemaker activity, we divided the parameter space as shown in Figure 9a. Red data indicate CL prolongation and blue data CL shortening compared to NG with added parasympathetic activity (CL=1.27s). Green data indicate CL>2s and purple data indicate invalid CL with no periodic pacemaker activity. At Ko=4mmol/L, all simulations result in valid periodic activity, with some CLs longer than 2s (see also Figure 8b). These are roughly confined to the area with g_{Kr}>0.9 and IVshift<-2mV. At Ko=3mmol/L, this area extends to g_{Kr}>0.8 and IVshift<-1mV (green circles). At Ko=3.7mmol/L, the model stops producing pacemaker activity around g_{Kr}=1 and IVshift=-3mV. At Ko=3mmol/L, this area extends to g_{Kr}>0.88 and IVshift<-1.8mV. Figure 9b shows examples of APs over 40s simulations. Baseline AP (CL=0.92s) is shown in the top row, followed by CL=2s in the second row and sinoatrial pauses in rows 3 to 5. The penultimate row shows the longest CL (around 25s), and the last row shows an example with no periodic pacemaker activity.
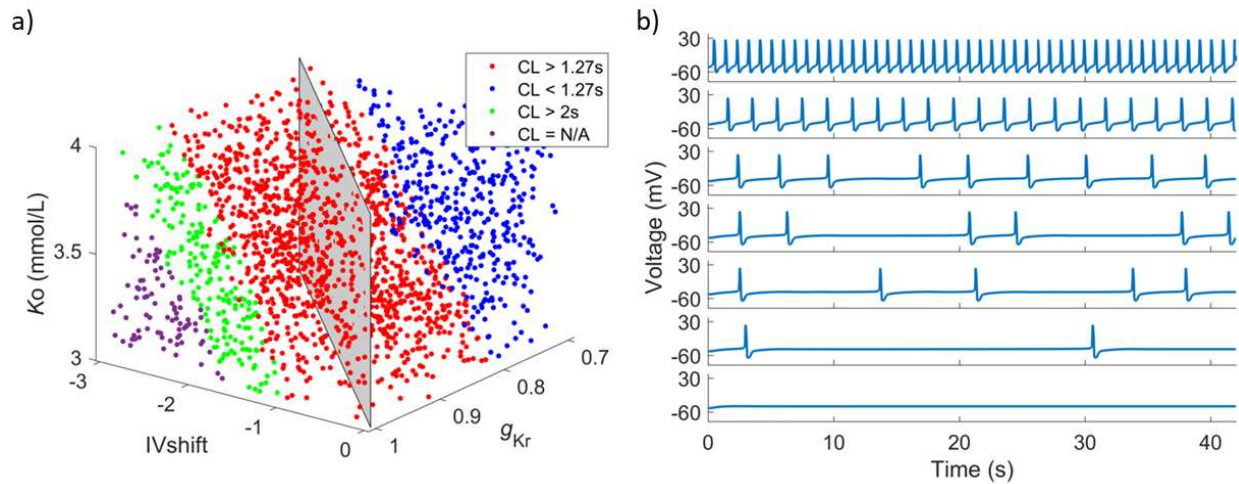
Figure 9: a) Classification of CL values produced with randomly sampled g_{Kr} [0.7, 1], IVshift [-3, 0]mV and Ko [3, 4]mmol/L when combined with parasympathetic activity. Red data indicate CL prolongation and blue data CL shortening versus baseline + parasympathetic activity (CL=1.27s). Green data indicate CL>2s and purple data invalid CL where the model did not produce periodic AP. b) Examples of simulated APs: baseline (CL=0.92s, top row), CL=2s (second row), sinoatrial pauses (rows 3-6) and no periodic AP (last row). Latin hypercube sampling, N=2000.

Discussion

In this first study investigating the effects of hypoglycaemia on the SA node electrophysiology we demonstrate the following findings. First, in response to hypoglycaemia, the reduced conductance of the hERG channel and the shift in its current-voltage relationship produce opposite effects on the pacemaker rate. When combined, they cancel each other out, resulting in a small decrease in heart rate. Second, mild hypokalaemia causes a slight decrease in heart rate. When combined with hypoglycaemia, there is a marked further decrease in heart rate. Third, hypoglycaemia combined with sympathetic activity enhances the effect of sympathetic activity by further increasing the heart rate compared to normoglycaemia. However, when hypoglycaemia is combined with hypokalaemia and sympathetic activity, the effect of sympathetic activity is diminished, causing a smaller increase in heart rate compared to that at normoglycaemia with added sympathetic activity. Fourth, hypoglycaemia enhances the effect of parasympathetic activity by causing a greater decrease in heart rate compared to normoglycaemia. Hypoglycaemia combined with hypokalaemia and parasympathetic activity causes a further marked reduction in heart rate, resulting in sinoatrial pauses, sinus arrest and block of pacemaker activity.

Combined, the above findings indicate that hypoglycaemia tends to decrease the pacemaker rate of the SA node. During experimental hypoglycaemia, where glucose was reduced in a controlled environment using insulin infusion, hypoglycaemia counterregulation caused a significant increase in circulating adrenaline and noradrenaline concentrations together with a significant decrease in potassium in healthy people (15) and in people with type 2 (15) and type 1 diabetes (14). Despite the significant increase in adrenaline and noradrenaline, there was a relatively small (about 3 bpm) increase in heart rate during hypoglycaemia compared to normoglycaemia (14,15). It is therefore possible, that decreased glucose and potassium levels counteract the effects of the autonomic nervous system at the level of the SA node. Robinson et al have reported the results of experimental studies in healthy subjects where they restored normal concentrations of potassium during both normoglycaemia and hypoglycaemia (14). They have shown that heart rate did not change during normoglycaemia after potassium has been added (Ko=3.6 vs 4mmol/L). On the other hand, there was an approximate 7 bpm increase in heart rate (61 vs 68bpm, +11%) when potassium was added (Ko=3.2 vs 3.9mmol/L) during hypoglycaemia. These data are in line with our findings that decreased potassium does not significantly affect the heart rate during normoglycaemia but causes a decrease in heart rate when combined with decreased glucose. For comparable values of Ko, our model shows a 2% higher heart rate during normoglycaemia and a 9% higher heart rate during hypoglycaemia.

In our study we demonstrate a potential mechanistic explanation for hypoglycaemia-induced bradycardia, which has been observed during clinical episodes in people with type 1 (29) and type 2 diabetes (22). We have undertaken several observational studies, where we compared rates of cardiac arrhythmia during spontaneous hypoglycaemia vs normoglycaemia. We observed increased incidences of bradycardia in people with type 1 diabetes (10), with type 2 diabetes (8) and with type 2 diabetes after discharge from ICU (11). However, increased rates of

bradycardia were only detected in a few individuals. We speculated that these effects are idiosyncratic and that mechanisms, other than those involved in hypoglycaemia counterregulation might contribute to the development of bradycardia (10,11,30). These could include autonomic dysfunction and/or abnormal and variable autonomic responses such as those observed during experimental hypoglycaemia, where early parasympathetic withdrawal was followed by parasympathetic reactivation during sustained hypoglycaemia (15). Nocturnal hypoglycaemia could also increase the risk as sleep and prone position diminish the sympathoadrenal responses during the night (31). Our findings that decreased blood glucose and potassium diminish the effect of the sympathetic activity and enhance the parasympathetic activity might further exacerbate the risk of bradycardia in the above cases.

To validate the responses of our model during hypoglycaemia, we used the heart rate differences between matched spontaneous hypoglycaemia and normoglycaemia episodes from our observational study in people with type 1 diabetes (10). We chose only nocturnal episodes due to diminished sympathoadrenal responses which in turn also cause a smaller reduction in Ko. Our computational model shows an approximate -1% decrease in heart rate during hypoglycaemia at Ko=4mmol/L. In our observational study there was a nonsignificant +2% increase in heart rate during hypoglycaemia vs normoglycaemia with a mean difference 1.5bpm (95%CI -1.3, 4.4)bpm. In a similar study, Koivikko et al (32) reported a +2% increase. Our computational data are within the confidence intervals of those from the above observational studies and the difference in trends could be partly due to counterregulatory sympathetic activation.

There are several conditions which could combine with the effects of hypoglycaemia to further promote decreased pacemaker rate at the SA node. Channelopathies, such as mutations in the HCN4, SCN5A and KCNQ1 genes, which encode ion currents I_f, I_{Na} and I_{Ks}, can lead to reduced pacemaker rate. In addition, remodeling of the I_f depolarisation current in trained athletes, which causes decreased resting heart rate and potential training-induced bradycardia (33) could lead to increased risk during hypoglycaemia. These cases could be further explored in the computational model of the human SA node as well as in observational or experimental hypoglycaemia studies.

In our model, we show a gradual increase in pacemaker rate with decreased g_{Kr} (Figure 2). This contradicts experimental data from animals, where selective blockage of I_{Kr} resulted in decreased rates in rabbit (34) and guinea pig (35) SA nodes. Due to lack of human experimental data to confirm our findings, we explored the reduction of g_{Kr} in a computational model of the rabbit SA node. We chose the Severi model (26), which is the parent model of the one used in this study. The AP waveforms and the relationship between g_{Kr} and CL are presented in Figure 10. CL is proportionally prolonged with reduced g_{Kr} (Figure 10a) and the pacemaker activity is abolished with complete block of I_{Kr} (g_{Kr}=0, Figure 10b). CL prolongation is accompanied by APD prolongation, elevation of MDP and decreased DDR. This is in line with experimental data from the rabbit SA node (34).
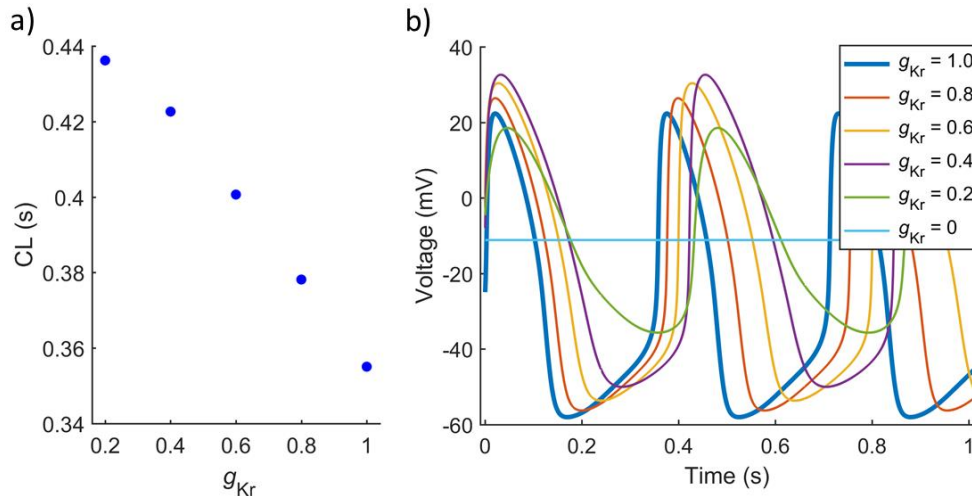
Figure 10: Effect of reduced g_{Kr} on CL in a computational model of rabbit SA node. a) CL is prolonged with the reduction in g_{Kr}. b) The corresponding AP waveforms indicate APD prolongation, elevated MDP and reduced DDR. The model doesn't generate AP with g_{Kr}=0.

In our human model, a reduction in g_{Kr} is accompanied by APD prolongation and elevation of MDP, as in the rabbit model. In contrast to the rabbit model, DDR increases in the human model (Table 1). One of the reasons for differences between the models is the roughly 2.5 times higher resting pacemaker rate in rabbits (CL=0.92s in human vs 0.36s in rabbit). While APD prolongation is similar in both models, this makes up a much bigger proportion of CL in the rabbit AP. In Figure 10b, APD prolongations are similar to the prolongations of CL while the opposite effects of elevated MDP and decreased DDR on CL seem to cancel each other out. In contrast, the duration of diastolic depolarisation is much longer in the human model, making the CL more susceptible to changes in DDR.

To further investigate the differences between DDR responses in both models, we compared the major currents responsible for diastolic depolarisation at g_{Kr}=1 vs g_{Kr}=0.5. In the rabbit model, the amplitude of I_f current is relatively high vs the other currents and its amplitude decreases by about 50% with reduced g_{Kr} (Supplementary Figure 2). Similarly, the amplitude of I_{NaCa} markedly decreases. In contrast, the amplitude of the I_f current is much smaller in absolute terms as well as relative to the other currents in the human model (Supplementary Figure 3). In addition, the amplitude of I_{NaCa} slightly increases with reduced g_{Kr}. These differential responses in currents, combined with the higher resting rate in rabbits could explain the differences between the g_{Kr} /CL relationship in humans vs rabbits. It is also possible that the decreased pacemaker rate in response to reduced g_{Kr} in rabbits contributes to the reduction of heart rate and occurrence of bradycardia during experimental hypoglycaemia in rabbits (16).

The key strength of our study is that we explored for the first time the electrophysiological effects of hypoglycaemia on the SA node. Furthermore, to mimic the physiological conditions in humans, we added the stimuli of hypokalaemia as well as sympathetic and parasympathetic stimulation. This approach overcomes some of the technical, biological and ethical constraints of in-vivo human and animal studies. One of the limitations of the study is the lack of detailed

experimental data on the effect of extracellular glucose concentration on cardiac cell electrophysiology. Zhang et al demonstrated the main effects of low glucose on the hERG channel (17), but experimental data at finer glucose increments would greatly improve the understanding of the balance between increased heart rate, caused by reduced conductance of the channel versus slowing of the rate caused by the shift in its current-voltage properties and how these relate to clinically relevant glucose levels. To the best of our knowledge, there is no evidence of any other cardiac ion channel being affected by hypoglycaemia.

Fabbri et al optimised their model to reproduce baseline electrophysiological characteristics from limited number of human experimental data and validated it against baseline heart rates observed in common ion channel mutations. Given the lack of experimental data, the model is not optimised and validated for variations in heart rate and altered extracellular ion concentrations. Loewe et al extended the Fabbri model to work at variable Ko concentrations by including a new formulation of I_{Kr}, where g_{Kr} is dependent on Ko (36). Their model showed a positive relationship between heart rate and Ko and they found that this was in disagreement with data from the general population, which showed a negative linear relationship. Our model, as the extended Fabbri model, shows a positive relationship between heart rate and Ko. This could mean that our model overestimates the CL at Ko=3mmol/L during normoglycaemia as well as with low glucose and in combination with parasympathetic activity. This behaviour of our model could be inherited from the parent model. Indeed, existing human atrial models show divergent and sometimes unphysiological responses to changing extracellular Ko (37) and the corresponding electrophysiological conditions remain to be explored. Finally, the Fabbri model offers selective activation of either sympathetic or parasympathetic activity. In reality, both branches of the autonomic system are continuously active and they complement each other to modulate the pacemaker rate. The responses of their combined activities and how these relate to their individual effects, observed in this study, remain to be investigated.

Conclusions

Computational modelling has the potential to clarify electro-pathophysiological effects of hypoglycaemia. We have shown that sinus arrest, a case of extreme bradycardia, is a plausible mechanism for SCD, possibly more probable than tachycardia during the night. Investigation of confounding factors that lead to development of abnormal cardiac responses, as well as modelling of different cardiac cells at different levels may help to identify individuals with diabetes who are at increased risk of sudden death due to sinus arrest during hypoglycaemia. This has important clinical implications because equivalent studies are not feasible or are challenging to perform in a clinical setting.

Author Contributions

AB, AI, SRH and RHC conceived the study; AB implemented the model, ran all the numerical experiments, and drafted the manuscript; RHC guided the numerical simulations and suggested ideas for figures; all authors then reviewed and contributed to development and finalisation of the manuscript.

Data Accessibility

Numerical data, source code of the model and the code to reproduce the figures are available in a github repository:
https://github.com/AlanBernjak/Bernjak_etal_Human_SAN_model_hypoglycaemia

References

1. Cryer PE. Glycemic goals in diabetes: trade-off between glycemic control and iatrogenic hypoglycemia. Diabetes. 2014 Jul;63(7):2188–95.

2. Gerstein HC, Miller ME, Byington RP, Goff DCJ, Bigger JT, Buse JB, et al. Effects of intensive glucose lowering in type 2 diabetes. N Engl J Med. 2008 Jun;358(24):2545–59.

3. The ORIGIN Trial Investigators. Does hypoglycaemia increase the risk of cardiovascular events? A report from the ORIGIN trial. Eur Heart J. 2013;34(40):3137–44.

4. Tattersall RB, Gill G V. Unexplained deaths of type 1 diabetic patients. Diabet Med. 1991;8(1):49–58.

5. Thordarson H, Søvik O. Dead in bed syndrome in young diabetic patients in Norway. Diabet Med. 1995 Sep;12(9):782–7.

6. Dahlquist G, Källén B. Mortality in childhood-onset type 1 diabetes: a population-based study. Diabetes Care. 2005 Oct;28(10):2384–7.

7. Secrest AM, Becker DJ, Kelsey SF, LaPorte RE, Orchard TJ. Characterizing sudden death and dead-in-bed syndrome in Type 1 diabetes: Analysis from two childhood-onset Type 1 diabetes registries. Diabet Med. 2011;28(3):293–300.

8. Chow E, Bernjak A, Williams S, Fawdry RA, Hibbert S, Freeman J, et al. Risk of cardiac arrhythmias during hypoglycemia in patients with type 2 diabetes and cardiovascular risk. Diabetes. 2014;63(5):1738–47.

9. Stahn A, Pistrosch F, Ganz X, Teige M, Koehler C, Bornstein S, et al. Relationship between hypoglycemic episodes and ventricular arrhythmias in patients with type 2 diabetes and cardiovascular diseases: Silent hypoglycemias and silent arrhythmias. Diabetes Care. 2014;37(2):516–20.

10. Novodvorsky P, Bernjak A, Chow E, Iqbal A, Sellors L, Williams S, et al. Diurnal Differences in Risk of Cardiac Arrhythmias during Spontaneous Hypoglycemia in Young People with Type 1 Diabetes. Diabetes Care. 2017;(1):1–8.

11. Ali Abdelhamid Y, Bernjak A, Phillips LK, Summers MJ, Weinel LM, Lange K, et al. Nocturnal Hypoglycemia in Patients With Diabetes Discharged From ICUs: A Prospective Two-Center Cohort Study. Crit Care Med. 2021;49(4):636–49.

12. Robinson RTCE, Harris ND, Ireland RH, Macdonald IA, Heller SR. Changes in cardiac repolarization during clinical episodes of nocturnal hypoglycaemia in adults with Type 1 diabetes. Diabetologia. 2004;47(2):312–5.

13. Marques JLB, George E, Peacey SR, Harris ND, Macdonald IA, Cochrane T, et al. Altered ventricular repolarization during hypoglycaemia in patients with diabetes. Diabet Med. 1997;14(8):648–54.

14. Robinson RTCE, Harris ND, Ireland RH, Lee S, Newman C, Heller SR. Mechanisms of abnormal cardiac repolarization during insulin-induced hypoglycemia. Diabetes. 2003 Jun;52(6):1469–74.

15. Chow E, Bernjak A, Walkinshaw E, Lubina-Solomon A, Freeman J, Macdonald IA, et al. Cardiac autonomic regulation and repolarization during acute experimental hypoglycemia in type 2 diabetes. Diabetes. 2017;66(5):1322–33.

16. Reno CM, Daphna-Iken D, Chen YS, VanderWeele J, Jethi K, Fisher SJ. Severe hypoglycemia-induced lethal cardiac arrhythmias are mediated by sympathoadrenal activation. Diabetes. 2013;62(10):3570–81.

17. Zhang Y, Han H, Wang J, Wang H, Yang B, Wang Z. Impairment of human ether-à-go-go-related gene (HERG) K+ channel function by hypoglycemia and hyperglycemia. Similar phenotypes but different mechanisms. J Biol Chem. 2003 Mar;278(12):10417–26.

18. Roden DM. Drug-induced prolongation of the QT interval. N Engl J Med. 2004 Mar;350(10):1013–22.

19. Heller SR, Cryer PE. Reduced neuroendocrine and symptomatic responses to subsequent hypoglycemia after 1 episode of hypoglycemia in nondiabetic humans. Diabetes. 1991 Feb;40(2):223–6.

20. Lee S, Harris ND, Robinson RT, Yeoh L, Macdonald IA, Heller SR. Effects of adrenaline and potassium on QTc interval and QT dispersion in man. Eur J Clin Invest. 2003;33(2):93–8.

21. Nordin C. The case for hypoglycaemia as a proarrhythmic event: Basic and clinical evidence. Diabetologia. 2010;53(8):1552–61.

22. Bolognesi R, Tsialtas D, Bolognesi MG, Giumelli C. Marked sinus bradycardia and QT prolongation in a diabetic patient with severe hypoglycemia. J Diabetes Complications. 2011;25(5):349–51.

23. Lindström T, Jorfeldt L, Tegler L, Arnqvist HJ. Hypoglycaemia and cardiac arrhythmias in patients with type 2 diabetes mellitus. Diabet Med. 1992 Jul;9(6):536–41.

24. Nordin C. The proarrhythmic effect of hypoglycemia: Evidence for increased risk from ischemia and bradycardia. Acta Diabetol. 2014;51(1):5–14.

25. Fabbri A, Fantini M, Wilders R, Severi S. Computational analysis of the human sinus node action potential: model development and effects of mutations. J Physiol [Internet]. 2017;595(7):2365–96.

26. Severi S, Fantini M, Charawi LA, Difrancesco D. An updated computational model of rabbit sinoatrial action potential to investigate the mechanisms of heart rate modulation. J Physiol. 2012;590(18):4483–99.

27. Rickert C, Proenza C. ParamAP: Standardized Parameterization of Sinoatrial Node Myocyte Action Potentials. Biophys J. 2017;113(4):765–9.

28. Kardalas E, Paschou SA, Anagnostis P, Muscogiuri G, Siasos G, Vryonidou A. Hypokalemia: a clinical update. Endocr Connect. 2018 Apr;7(4):R135–46.

29. Gill G V, Woodward A, Casson IF, Weston PJ. Cardiac arrhythmia and nocturnal hypoglycaemia in type 1 diabetes--the "dead in bed" syndrome revisited. Diabetologia.

2009 Jan;52(1):42–5.

30.   Campbell M, Heller SR, Jacques RM. Diurnal differences in risk of cardiac arrhythmias during spontaneous hypoglycemia in young people with type 1 diabetes. Diabetes care 2017;40:655-662. Diabetes Care. 2018;41(4):e65–6.

31.   Jones TW, Porter P, Sherwin RS, Davis EA, O'Leary P, Frazer F, et al. Decreased epinephrine responses to hypoglycemia during sleep. N Engl J Med. 1998 Jun;338(23):1657–62.

32.   Koivikko ML, Tulppo MP, Kiviniemi AM, Kallio MA, Perkiömäki JS, Salmela PI, et al. Autonomic cardiac regulation during spontaneous nocturnal hypoglycemia in patients with type 1 diabetes. Diabetes Care. 2012;35(7):1585–90.

33.   D'souza A, Bucchi A, Johnsen AB, Logantha SJRJ, Monfredi O, Yanni J, et al. Exercise training reduces resting heart rate via downregulation of the funny channel HCN4. Nat Commun. 2014;5.

34.   Kodama I, Boyett MR, Nikmaram MR, Yamamoto M, Honjo H, Niwa R. Regional differences in effects of E-4031 within the sinoatrial node. Am J Physiol. 1999 Mar;276(3):H793-802.

35.   Matsuura H. Rapidly and slowly activating components of delayed rectifier K+ current in guinea-pig sino-atrial node pacemaker cells. J Physiol. 2002;540(3):815–30.

36.   Loewe A, Lutz Y, Nairn D, Fabbri A, Nagy N, Toth N, et al. Hypocalcemia-Induced Slowing of Human Sinus Node Pacemaking. Biophys J. 2019;117(12):2244–54.

37.   Passini E, Genovesi S, Severi S. Human atrial cell models to analyse haemodialysis-related effects on cardiac electrophysiology: Work in progress. Comput Math Methods Med. 2014;2014:291598.